



ACADEMIC  
PRESS

Available online at [www.sciencedirect.com](http://www.sciencedirect.com)

SCIENCE @ DIRECT®

Journal of Solid State Chemistry 171 (2003) 345–348

JOURNAL OF  
SOLID STATE  
CHEMISTRY

<http://elsevier.com/locate/jssc>

# Structure and magnetism of $\text{Eu}_{1-x}\text{Dy}_x\text{TiO}_3$

K. Yoshii,<sup>a,\*</sup> M. Mizumaki,<sup>b</sup> A. Nakamura,<sup>c</sup> and H. Abe<sup>d</sup>

<sup>a</sup>Japan Atomic Energy Research Institute, Mikazuki, Hyogo 679-5148, Japan

<sup>b</sup>Japan Synchrotron Radiation Institute, Mikazuki, Hyogo 679-5198, Japan

<sup>c</sup>Japan Atomic Energy Research Institute, Tokai, Ibaraki 319-1195, Japan

<sup>d</sup>National Institute for Materials Science, Tsukuba, Ibaraki 305-0047, Japan

Received 17 April 2002; received in revised form 25 August 2002; accepted 28 August 2002

## Abstract

Structure and magnetism have been investigated for perovskite  $\text{Eu}_{1-x}\text{Dy}_x\text{TiO}_3$ . It is known that while  $\text{EuTiO}_3$  ( $x = 0$ ) exhibits antiferromagnetism below  $\sim 6$  K,  $\text{DyTiO}_3$  ( $x = 1$ ) becomes a ferrimagnet below  $\sim 64$  K. The crystal structures are assigned to be cubic and orthorhombic for  $x \leq 0.3$  and  $x \geq 0.4$ , respectively. Magnetic transitions are observed for all the compounds. The valence of Eu is assumed to be  $2+$  in the solid solutions as well on the basis of inverse susceptibility data. Characteristic phenomena, such as the metallic ferromagnetism for  $0.1 \leq x \leq \sim 0.5$ , are likely due to a mixed or an intermediate valence state of Ti.

© 2003 Elsevier Science (USA). All rights reserved.

**Keywords:** Titanium oxide; Perovskite; Europium; Dysprosium; Ferrimagnetism

## 1. Introduction

Lanthanide perovskite titanates  $Ln\text{TiO}_3$  have an orthorhombic perovskite structure for all lanthanides except  $Ln = \text{Eu}$  [1–3]. Whereas the compounds with  $Ln = \text{La}–\text{Sm}$  show a so-called canted-antiferromagnetic order of  $\text{Ti}^{3+}$  localized moments ( $3d^1$ ,  $S = \frac{1}{2}$ ) between  $\sim 50$  and  $140$  K, the ferrimagnetic order of the  $\text{Ti}^{3+}$  and  $Ln^{3+}$  sublattices takes place below Curie temperatures ( $T_C$ ) of  $\sim 30–64$  K for the heavier lanthanides of  $Ln = \text{Gd}–\text{Tm}$  [2]. All of these compounds are the Mott–Hubbard-type insulators owing to strong Coulomb repulsion between the  $\text{Ti}3d$  electrons.  $\text{EuTiO}_3$  has a cubic perovskite structure and is also insulating, where the Ti ion is in a valence state of  $4+$  ( $3d^0$ ) and has no localized moment [4,5]. The  $\text{Eu}^{2+}$  moments ( $4f^7$ ) antiferromagnetically order below  $\sim 6$  K.

Recently, magnetic and transport properties were reported for La- and Gd-substituted  $\text{EuTiO}_3$  [6]. In the former system, where the  $\text{La}^{3+}$  ion has no localized  $4f$  moment, the properties were investigated for low La-substitutions of 10% and 20%. An appreciable enhancement of magnetization at low temperatures was ascribed to the ferromagnetism of the  $\text{Eu}^{2+}$  moment.

For the substitution of  $\text{Gd}^{3+}$  having the same  $4f^7$  configuration as  $\text{Eu}^{2+}$ , the  $\text{Eu}_{1-x}\text{Gd}_x\text{TiO}_3$  samples were prepared for the large substitutions of  $x = 0.5$  and  $0.7$ . Oscillation of  $T_C$  against  $x$  was explained in connection with a Ruderman–Kittel–Kasuya–Yosida (RKKY)-type magnetic interaction between the lanthanide moments via  $\text{Ti}3d$  conduction electrons. In this work, structural and magnetic properties were studied for the substitution of a heavier lanthanide Dy for Eu. The samples were prepared in a wide composition region of  $0 \leq x \leq 1$  for  $\text{Eu}_{1-x}\text{Dy}_x\text{TiO}_3$ . The end compound  $\text{DyTiO}_3$  ( $x = 1$ ) exhibits the highest  $T_C$  of  $64$  K among ferrimagnetic  $Ln\text{TiO}_3$  compounds [2].

## 2. Experimental procedures

The  $\text{Eu}_{1-x}\text{Dy}_x\text{TiO}_3$  samples ( $0 \leq x \leq 1$ ), where an increment of  $x$  was  $0.1$ , were prepared by a solid-state reaction in a vacuum. Stoichiometric mixtures of  $Ln_2\text{O}_3$  ( $Ln = \text{Eu}$  and  $\text{Dy}$ ) and  $\text{Ti}_2\text{O}_3$  (3N-4N, Soekawa) were thoroughly ground, pressed into pellets, and fired at  $1500–1550^\circ\text{C}$  for  $12–24$  h. The firing was repeated two to three times with intermediate grindings. Some of the compounds were prepared twice and found to show reproducible structural and magnetic properties. The

\*Corresponding author. Fax: +81-791-58-2740.

E-mail address: [yoshiike@spring8.or.jp](mailto:yoshiike@spring8.or.jp) (K. Yoshii).

actual oxygen contents  $y$  were 3.00–3.03(2) in  $\text{Eu}_{1-x}\text{Dy}_x\text{TiO}_3$  from thermogravimetry. For brevity, the compounds will be denoted as  $\text{Eu}_{1-x}\text{Dy}_x\text{TiO}_3$ . Their crystal structures were determined by powder X-ray diffraction (XRD) using  $\text{CuK}\alpha$  radiation. The XRD patterns were refined by the Rietveld method using the program RIETAN-2000 [7]. Magnetic properties were measured in a SQUID magnetometer (Quantum Design MPMS) between 4.5 and 400 K. For  $\text{EuTiO}_3$  only, the measurements were done down to 2 K because of the low Néel temperature of  $\sim 6$  K. DC magnetic susceptibility–temperature ( $\chi - T$ ) curves were measured with an applied field ( $H$ ) of 100 Oe. The susceptibility is given by  $\chi = M/H$  ( $M$ : magnetization). Isothermal magnetization was measured at 4.5 K within applied fields of  $\pm 50,000$  Oe. Electrical resistivity was measured by means of the DC four-probe method between 4.2 K and room temperature.

### 3. Results and discussion

Fig. 1 shows the XRD patterns of  $\text{Eu}_{0.6}\text{Dy}_{0.4}\text{TiO}_3$  ( $x = 0.4$ ). The experimental pattern could be fitted assuming the orthorhombic structure of  $Pnma$  as in the case of  $\text{DyTiO}_3$  [2,3]. The lattice parameters for  $0 \leq x \leq 1$  are plotted in Fig. 2. All the patterns showed the samples to be in a single phase. The crystal structure changes from cubic to orthorhombic at  $x = 0.3$ – $0.4$ . In the cubic region, a space group  $Pm\bar{3}m$  was adopted. Each lattice parameter changes almost continuously against  $x$ , which indicates the formation of a solid solution in the whole compositions. It was also found that the Ti–O–Ti angle decreased from  $\sim 160^\circ$  to  $\sim 140^\circ$  with increasing  $x$  over the interval  $0.4 \leq x \leq 1$ . As the

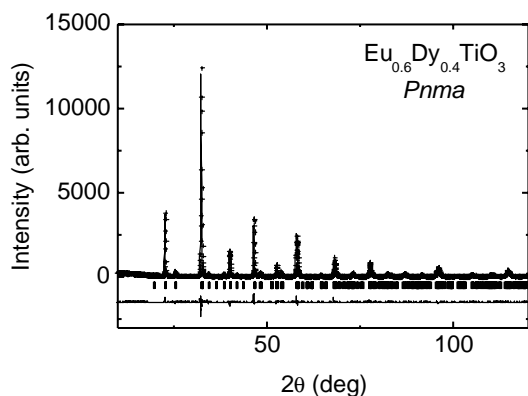


Fig. 1. XRD patterns at room temperature for  $\text{Eu}_{0.6}\text{Dy}_{0.4}\text{TiO}_3$  (space group  $Pnma$ ). The observed and calculated patterns are shown by cross marks and the top solid line, respectively. The vertical markers stand for the angles of Bragg reflections. The lowest solid line represents the difference between the calculated and observed intensities. The lattice parameters are  $a = 5.5221(3)$  Å,  $b = 7.7653(4)$  Å, and  $c = 5.4791(3)$  Å. Reliability factors ( $R$ ) are  $R_{\text{wp}} = 13.0\%$ ,  $R_c = 8.22\%$ ,  $R_1 = 4.72\%$ , and  $R_F = 2.99\%$ .

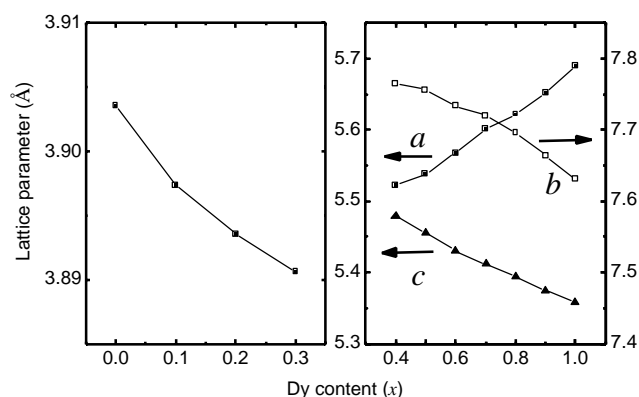


Fig. 2. Lattice parameters for  $\text{Eu}_{1-x}\text{Dy}_x\text{TiO}_3$  plotted as a function of the Dy content ( $x$ ). The Rietveld refinement was done assuming cubic  $Pm\bar{3}m$  and orthorhombic  $Pnma$  for  $x \leq 0.3$  and  $x \geq 0.4$ , respectively.

ionic radii of  $\text{Eu}^{2+}$  ( $4f^7$ ) and  $\text{Eu}^{3+}$  ( $4f^6$ ) are larger than that of  $\text{Dy}^{3+}$  ( $4f^9$ ) [8], the valence of the Eu ion cannot be determined from this data alone.

Figs. 3a and b show the  $\chi - T$  curves for  $x \leq 0.4$  and  $x \geq 0.5$ , respectively. Though both FC (field-cooled) and ZFC (zero-field-cooled) curves were measured, only the former curves are presented here. For all the curves, the ZFC susceptibilities were smaller than the FC susceptibilities below the transition temperatures. The difference between the FC and ZFC susceptibilities was small (typically by 2–3%) for the Eu-rich region (for  $x < \sim 0.6$ ) but fairly large for the Dy-rich region (for  $x > \sim 0.7$ ), where susceptibility cusps were observed below transition temperatures. This result is relevant to an increase in coercivity with increasing Dy content (see Fig. 4 for brevity). The figures confirm that  $\text{EuTiO}_3$  and  $\text{DyTiO}_3$  exhibit antiferromagnetic and ferrimagnetic orders below  $\sim 6$  and  $\sim 64$  K, respectively. Fig. 3a also shows that low-temperature susceptibilities are considerably enhanced by a slight  $\text{Dy}^{3+}$  substitution of 10%. A plateau of susceptibility below  $\sim 10$  K in the inset for  $x = 0.2$  is a similar phenomenon to that for  $\text{Eu}_{0.9}\text{La}_{0.1}\text{TiO}_3$  [6]. This plateau disappears at  $x \geq 0.4$ . The temperature derivative of inverse susceptibility for  $x = 0.1$ – $0.5$  provided transition temperatures between  $\sim 9$  and  $\sim 12$  K, the tendency of which against  $x$  was not observed. Low-temperature susceptibilities show a rough tendency to decrease with increasing  $x$  from 0.1 to 0.6. The compounds with  $x \geq 0.6$ – $0.7$  exhibit another magnetic transition above  $\sim 30$  K (Fig. 3b), as pointed out by an arrow. This transition temperature seems to become higher with increasing  $x$  from 0.6 to 1. At  $x = 1$  ( $\text{DyTiO}_3$ ), the transition manifests itself as the ferrimagnetic transition at 64 K. From this behavior, a ferrimagnetic order is assumed to be responsible for the transitions in  $x \geq 0.6$ . For  $x \geq 0.7$ , the low-temperature susceptibilities are enhanced at  $x = 0.8$  and  $0.9$  and are decreased again at  $x = 1$ . AC magnetic susceptibility

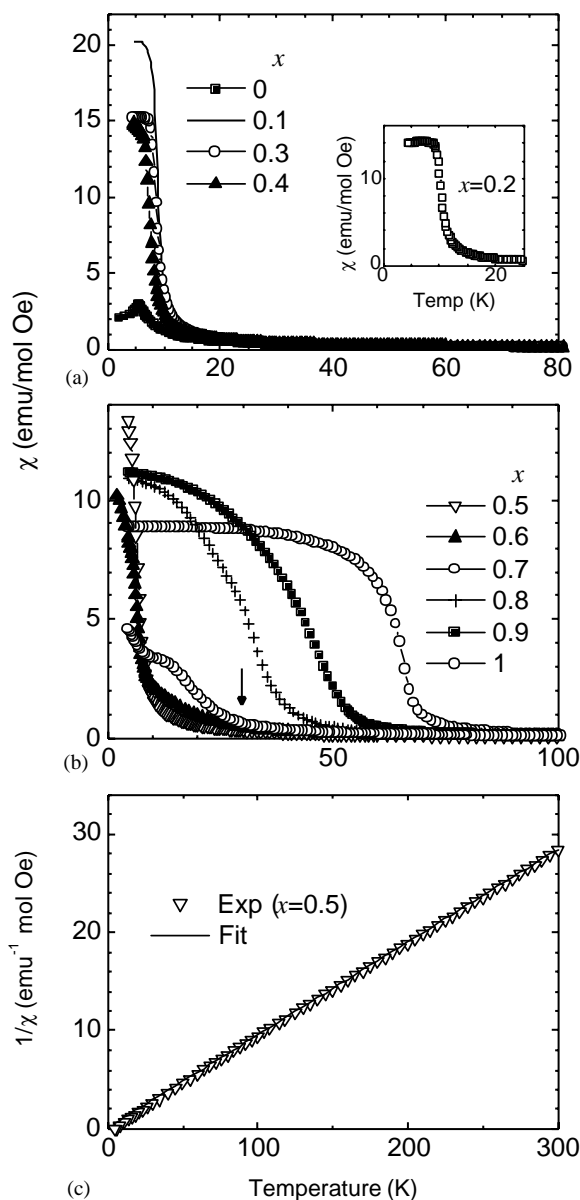


Fig. 3. (a) FC  $\chi$ - $T$  curves for  $\text{Eu}_{1-x}\text{Dy}_x\text{TiO}_3$  for  $x \leq 0.4$  measured with  $H = 100$  Oe. A curve for  $x = 0.2$  is displayed in the inset to show details around the transition temperature. (b) The same as (a) for  $x \geq 0.5$ . An arrow points out a magnetic transition for  $x = 0.6$ . (c) Inverse susceptibility plotted against the temperature for  $x = 0.5$ . The Curie-Weiss fit for the experimental curve (Exp) is shown as Fit.

measurements indicated that the frequency dependence of susceptibility, as seen in spin-glasses [10], also occurred for  $x = 0.7$  and  $0.8$  (not shown). This behavior indicates the presence of magnetic frustration.

Fig. 3c shows inverse susceptibility plotted as a function of the temperature for  $x = 0.5$ . The experimental (Exp) curve obeys the Curie-Weiss (CW) law above  $\sim 50$  K. An effective paramagnetic moment calculated from this data was  $9.21 \pm 0.50 \mu_B$ /unit formula. This value is close ( $\sim 98\%$ ) to that calculated from free-ion  $\text{Eu}^{2+}$  ( $7.9 \mu_B$  [9]),  $\text{Dy}^{3+}$  ( $10.6 \mu_B$  [9]), and spin-only  $\text{Ti}^{3+}$  ( $1.73 \mu_B$ ). If the Eu ion has the valence

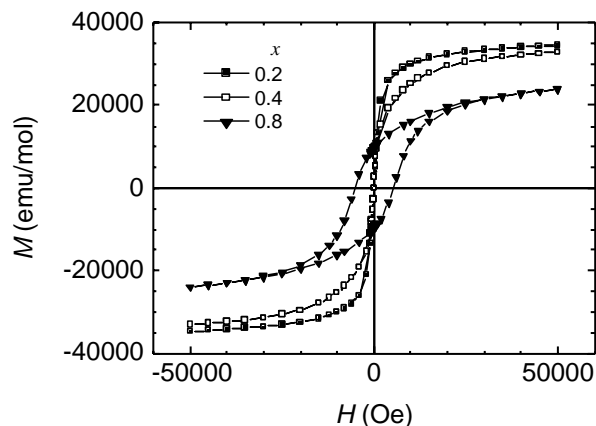


Fig. 4. Isothermal magnetization ( $M$ ) at 4.5 K plotted against the applied field ( $H$ ) for  $\text{Eu}_{0.8}\text{Dy}_{0.2}\text{TiO}_3$  ( $x = 0.2$ ),  $\text{Eu}_{0.6}\text{Dy}_{0.4}\text{TiO}_3$  ( $x = 0.4$ ), and  $\text{Eu}_{0.2}\text{Dy}_{0.8}\text{TiO}_3$  ( $x = 0.8$ ).

of  $3+$  ( $3.4$ – $3.5 \mu_B$  [9]), the calculated moment is  $\sim 8.08 \mu_B$ /unit formula. Thus, the valence of Eu is assumed to be  $2+$  rather than  $3+$ . The fact that the experimental value is smaller than the calculated value may be ascribed to crystal-field effects. The CW fit could be done on the assumption of the  $2+$  valence of Eu for all samples except for  $x = 1$ . Therefore, the valence of Ti in the solid solution changes from  $4+$  to  $3+$  with increasing  $x$ . The deviation from the CW law below  $\sim 50$  K in the figure implies an onset of magnetic correlation. The Weiss temperature ( $\theta$ ) was calculated to be  $0 \pm 1$  K, suggesting the presence of a very weak magnetic interaction. The  $\theta$  value changed between  $\sim -8$  and  $\sim +5$  K over the interval  $0 \leq x \leq 1$  and showed no apparent composition dependence.

Fig. 4 shows isothermal magnetization plotted against the applied field for  $\text{Eu}_{0.8}\text{Dy}_{0.2}\text{TiO}_3$  ( $x = 0.2$ ),  $\text{Eu}_{0.6}\text{Dy}_{0.4}\text{TiO}_3$  ( $x = 0.4$ ), and  $\text{Eu}_{0.2}\text{Dy}_{0.8}\text{TiO}_3$  ( $x = 0.8$ ) at 4.5 K. The ferromagnetic saturation of magnetization is seen in each curve. Analogous curves were obtained for all the other compounds including  $\text{EuTiO}_3$ , revealing that the antiferromagnetic order of  $\text{Eu}^{2+}$  is readily collapsed by high magnetic fields. For  $x \leq \sim 0.6$ , magnetization at 50,000 Oe corresponded to the  $\sim 6$ – $7 \mu_B$ /formula unit and exhibited no apparent composition dependence. Coercivity was quite small (typically  $\sim 20$  Oe) for the Eu-rich compounds ( $x \leq \sim 0.5$ ), plausibly owing to the zero orbital moment of a free-ion  $\text{Eu}^{2+}$ . When  $x$  increases above  $\sim 0.7$ , this value tends to increase (up to 20,000 Oe for  $x = 1$ ), as is demonstrated from the data for  $x = 0.8$ .

Fig. 5 shows electrical resistivity as a function of the temperature for  $\text{Eu}_{0.8}\text{Dy}_{0.2}\text{TiO}_3$  ( $x = 0.2$ ),  $\text{Eu}_{0.3}\text{Dy}_{0.7}\text{TiO}_3$  ( $x = 0.7$ ), and  $\text{DyTiO}_3$  ( $x = 1$ ). In Fig. 5a,  $\text{Eu}_{0.8}\text{Dy}_{0.2}\text{TiO}_3$  exhibits metallic behavior similar to that of  $\text{Eu}_{0.9}\text{La}_{0.1}\text{TiO}_3$  [6]. The drop of resistivity below  $\sim 10$  K (inset) coincides with the ferromagnetic transition seen in Fig. 3a. The other two compounds are

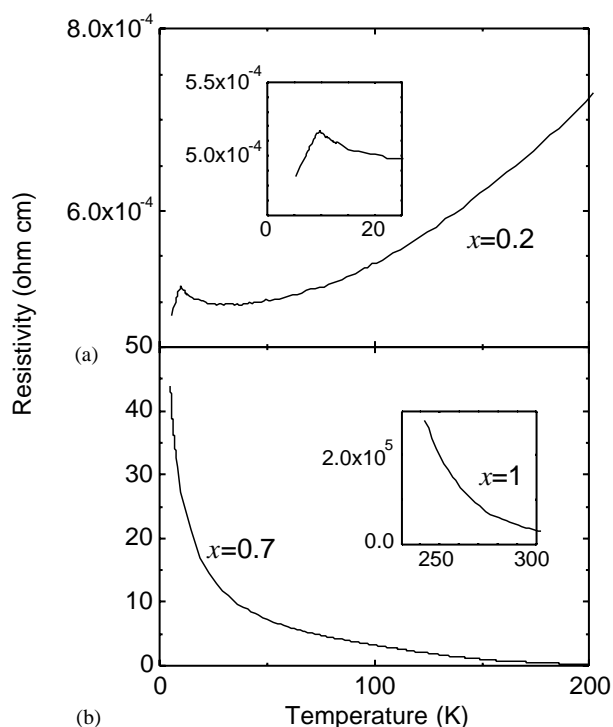


Fig. 5. Electrical resistivity plotted against the temperature for (a)  $\text{Eu}_{0.8}\text{Dy}_{0.2}\text{TiO}_3$  ( $x=0.2$ ). The inset shows the temperature region around the magnetic transition (Fig. 3a). (b) The same as Fig. 5a for  $\text{Eu}_{0.3}\text{Dy}_{0.7}\text{TiO}_3$  ( $x=0.7$ ) and  $\text{DyTiO}_3$  ( $x=1$ , inset).

insulating, as shown in Fig. 5b. The activation energy of  $\text{DyTiO}_3$  was calculated to be  $\sim 240$  meV at around room temperature, and a measurement below  $\sim 240$  K could not be done because of the very large resistance. The fact that the activation energy is larger than that for  $\text{LnTiO}_3$ , which contains lighter  $\text{Ln}^{3+}$  ions [1], is due to a smaller electron transfer that arises from a narrowing of the Ti–O–Ti angle. Roughly, the resistivities for  $x \geq 0.1$  have been found to increase with increasing  $x$ .

These experimental data can be qualitatively understood as follows, taking into account the results from previous work [6]. Upon the  $\text{Dy}^{3+}$  substitution, the nonmagnetic  $\text{Ti}^{4+}$  ions are partially converted into a magnetic  $\text{Ti}^{3+}$  state due to charge compensation. This mixed or intermediate valence state introduces charge carriers in a  $\text{Ti}3d$  band, as shown in Fig. 5, which is the case for other titanates such as  $\text{La}_{1-x}\text{Sr}_x\text{TiO}_3$  [11]. It is possible that the magnetic interactions between the lanthanide moments arise from an RKKY-type mechanism mediated by the  $\text{Ti}3d$  conduction electrons. No apparent relationship in the transition temperatures (10–12 K) and the Weiss temperatures ( $\sim -8$  and  $\sim +5$  K)

for  $x \leq \sim 0.5$  is relevant, since this type of interaction changes both its sign and strength depending on parameters such as the Fermi energy and lattice length. When  $x$  is increased, this interaction becomes weaker because of the enhancement of electron correlation leading to the localization of  $\text{Ti}3d$  electrons [11]. Localization is also induced by the narrowing of the Ti–O–Ti angle shown from the XRD data noted earlier. Thus, in the Dy-rich region, the magnetic interaction is the result of the electron hopping of  $\text{Ti}3d$ , as is the case in insulating oxides. The compounds with  $x \geq \sim 0.6$  showing transitions above  $\sim 30$  K (Fig. 3b) seem to be located around a boundary where the competition between the itinerancy and localization of  $\text{Ti}3d$  appears. Both the change of low-temperature susceptibilities against  $x$  and the spin-glass state are probably associated with this competition, for which there is, at present, no further explanation. The smaller low-temperature susceptibilities for  $x=1$  than for  $x=0.8$  and  $0.9$  plausibly indicate that the ferrimagnetic coupling between the  $\text{Ln}^{3+}$  and  $\text{Ti}^{3+}$  moments becomes stronger due to the increase in the amount of the magnetic  $\text{Ti}^{3+}$  ion. To confirm this scenario, a comparison with  $\text{Eu}_{1-x}\text{Yb}_x\text{TiO}_3$  or  $\text{Eu}_{1-x}\text{Lu}_x\text{TiO}_3$  may be useful because of the small magnetic moments of  $\text{Yb}^{3+}$  ( $4f^{13}$ ,  $4.5 \mu_B$  [9]) and  $\text{Lu}^{3+}$  ( $4f^{14}$ ,  $0 \mu_B$ ), which allow for a more accurate estimation of the magnetic effects from Ti. For this purpose, a preparation method for single-phase  $\text{YbTiO}_3$  and  $\text{LuTiO}_3$  must be established [2]. A proper treatment for describing localization effects should also be developed for a more detailed and quantitative discussion of the phenomena observed.

## References

- [1] J.E. Greedan, *J. Less-Common Metals* 111 (1985) 335–345.
- [2] C.W. Turner, J.E. Greedan, *J. Solid State Chem.* 34 (1980) 207–213.
- [3] C.W. Turner, M.F. Collins, J.E. Greedan, *J. Magn. Magn. Mater.* 23 (1981) 265–273.
- [4] J.E. Greedan, G.J. McCarthy, *Mater. Res. Bull.* 7 (1972) 531–541.
- [5] C.-L. Chien, S. DeBenedetti, F. De, S. Barros, *Phys. Rev. B* 10 (1974) 3913–3922.
- [6] T. Katsufuji, Y. Tokura, *Phys. Rev. B* 60 (1999) R15021–R15023.
- [7] F. Izumi, T. Ikeda, *Mater. Sci. Forum* 321–324 (2000) 198–204.
- [8] R.D. Shannon, *Acta. Crystallogr. A* 32 (1976) 751–767.
- [9] J.H. Van Vleck, *The Theory of Electric and Magnetic Susceptibilities*, Oxford University Press, London, 1965.
- [10] J.A. Mydosh, *Spin Glasses*, Taylor and Francis, London, 1993.
- [11] Y. Tokura, Y. Taguchi, Y. Okada, Y. Fujishima, T. Arima, K. Kumagai, Y. Iye, *Phys. Rev. Lett.* 70 (1993) 2126–2129.